

Superfluidity of light in nematic liquid crystals

Tiago D. Ferreira,^{*} Nuno A. Silva, and A. Guerreiro

*Departamento de Física e Astronomia da Faculdade de Ciências da Universidade do Porto,
Rua do Campo Alegre 687, 4169-007 Porto, Portugal
and INESC TEC, Centre of Applied Photonics, Rua do Campo Alegre 687, 4169-007 Porto, Portugal*



(Received 8 June 2018; published 13 August 2018)

Optical analog experiments have captured a lot of interest in recent years by offering a strategy to test theoretical models and concepts that would be otherwise untestable. The approach relies on the similarity between the mathematical model for light propagation in nonlinear optical media and the model to be mimicked. In particular, the analogy between light and a quantum fluid with superfluidlike properties has been studied extensively. Still, while most of these studies use thermo-optical media to perform these experiments, the possibility of using nematic liquid crystals to perform such optical analog experiments remains to be analyzed. This work explores how this medium can constitute an alternative to materials more commonly used in optical analogs, such as thermo-optical media, and how its tunable properties can be advantageous to explore and better control fluidlike properties of light. Moreover, we explore the analogy between the propagation of light and a quantum fluid, and propose a pump-probe experiment to measure the dispersion relation of the superfluid analog.

DOI: [10.1103/PhysRevA.98.023825](https://doi.org/10.1103/PhysRevA.98.023825)

I. INTRODUCTION

Optical analogs appear as a versatile test bed for theories that otherwise cannot be validated experimentally. In the particular case of many-body physics, photons are interpreted as particles that can have strong interactions via the nonlinear optical properties of the media. Recent examples of this approach include analogs spanning from superfluids [1,2] to boson stars [3] and others [4–8]. However, adjusting the features of the mimicker to match those of the mimicked system requires a precise control of the optical properties of the former, something which lacks in the materials normally used to produce optical analogs, such as nonlinear crystals or thermo-optical media. In this context, nematic liquid crystals appear as a tunable alternative to these types of materials.

Nematics liquid crystals (NLCs) consist of elongated molecules that in the nematic phase tend to align along the molecular director. Their optical properties are related with the alignment between the direction of polarization of the electric field and the orientation of the molecules, and in general they exhibit strong nonlocal effects [9–11]. These effects are typically nonlinear and, contrary to the simple Kerr effect, depend not only on the local intensity but also on the intensity in neighboring regions. These characteristics have been studied extensively in the last decade as they introduce nontrivial opportunities in the field of nonlinear optics. Indeed, materials with nonlocal optical response, such as nematic liquid crystals, have been proposed as support media for observing a plethora of phenomena, from the realization of bright multidimensional spatial [12,13], spatiotemporal [14], and vector solitons [15], to geometric phase-controlled wave guiding [16] and optical spontaneous symmetry breaking [17], just to name a few.

When compared with other nonlocal optical media, such as thermo-optical materials, NLCs can offer higher nonlinearities [18–22] with lower absorption effects [10]. Moreover, this nonlocal response can be controlled externally, for example by applying a quasistatic electric field or by adjusting the anchoring boundary conditions, which provides an important source of tunability for the system [21–27] and can play an important role in the development of optical analog experiments with NLCs, which to our best knowledge remains to be explored.

In this work we theoretically explore the potential use of self-defocusing nematic liquid crystals [22,28,29] in the context of optical analog experiments. In particular, we pursue a recent approach that establishes an analogy between light and a quantum fluid [1,30–33] which stems from the hydrodynamic interpretation of light provided by the Madelung transformation. In this interpretation, the intensity and the spatial gradient of the phase of light are mapped into the density and velocity of a fluid [34], respectively, while the propagation distance plays the role of the temporal coordinate, such that each transverse slice along the optical axis corresponds to an instantaneous state of the mimicked system. Fluids of light have captured much attention in recent years and their superfluidlike behavior has been predicted and observed either indirectly, via the measurement of the characteristic Bogoliubov-like dispersion relation [1], or directly, via the observation of vortex nucleation [33], persistent currents [2], and drag-force cancellation [35]. This phenomenology depends only on the type of nonlinearity of the media, which means that it can be reproduced using a multitude of distinct support systems, which include the more controllable nematic liquid crystals.

This paper is organized as follows. In Sec. II we consider the theoretical model that describes the propagation of a light beam inside of a nematic liquid crystal in the (1+1)D scheme, corresponding to one spacial and one temporal dimension in the mimicked system, discuss the hydrodynamic model

^{*}tiagodsferrera@hotmail.com

of the system, and obtain the dispersion relation for small excitations using the Bogoliubov theory. In Sec. III we propose an experiment based on a pump-probe scheme to measure the dispersion relation and present numerical simulations of the experiment. The numerical simulations show that our methodology is robust even in the presence of noise, and extends the validity of the existing methods into the deep sonic regime. Finally, we discuss our results in Sec. IV.

II. PHYSICAL MODEL

Nematic liquid crystals can behave either as self-focusing or as self-defocusing media [28]. In the former, the nonlocal nonlinearity originates from the reorientation of the molecules due to a light beam, whereas the latter can be obtained by the addition of dopants with a negative Janossy coefficient, by NLCs with negative dielectric anisotropy ($n_{\perp} > n_{\parallel}$) such as *p*-methoxybenzylidene-*p'*-*n*-butylaniline (MBBA) liquid crystal [11], or by exploiting the thermo-optical response of the medium [28].

A. Equations (1+1)D for self-defocusing NLCs

In typical experiments, a beam of polarized light propagates along the optical axis z through a cell filled with a nematic liquid crystal, characterized by a molecular director in the y - z plane. The molecular director can be given a pretilt of θ_0 relative to the optical axis through the combination of a quasistatic electric field and special anchoring boundary conditions, for example [18]. The electric field of the beam exerts a torque on the molecules that can gyrate the molecular director by an extra rotation of θ from the initial orientation θ_0 . However, for this reorientation to occur, the field must be sufficiently strong to overcome the Fréedericksz threshold associated with the rotational inertia of the molecules [18]. It is therefore important to lower this threshold by adjusting θ_0 and thus avoid using excessive optical power that can lead to thermo-optical effects [18].

The propagation of an optical beam in this medium can be described using the paraxial approximation and neglecting the birefringence walk-off. In situations with strong nonlocal effects, the extra rotation θ is small and the propagation of light can be modeled by a Schrödinger-like equation coupled to an elliptic equation describing the alignment of the molecules with the field [10,22,29], and given by

$$i \frac{\partial E}{\partial z} + \frac{1}{2} \frac{\partial^2 E}{\partial x^2} - 2\theta E = 0, \quad (1)$$

$$v \frac{\partial^2 \theta}{\partial x^2} - 2q\theta = -2|E|^2, \quad (2)$$

in normalized units, where E is the complex envelope of the beam and $q = q(\theta_0)$ is proportional to the square of the static electric field that pretilts the molecule director. Also, v is the normalized elastic coefficient and measures the strength of the response of system, with $v \rightarrow 0$ indicating a local medium, whereas a larger v corresponds to a highly nonlocal NLC [22,36]. The degree of nonlocality can be varied from local to nonlocal by changing the pretilt angle via a bias voltage [20,37].

Equations (1) and (2) constitute the celebrated Schrödinger-Newton system of equations [38–40] and describe the

propagation of light in a NLC. Interestingly, this mathematical system also describes a range of phenomena in physics, ranging from gravitational models to quantum fluids. The similarities between these models motivated the proposal and implementation of optical analog experiments in recent years [1,3,4,8]. The common approach is to use thermo-optical materials that provide the nonlocal nonlinearities necessary to emulate the Schrödinger-Newton equations [1,3]. Unfortunately, it is difficult to adjust the nonlinear properties of thermo-optical materials and thus to explore the full range of dynamical behavior that characterizes these equations and the corresponding mimicked systems. When compared with thermo-optical materials, NLCs have the advantage, in that they can be more easily tuned by simple adjusting of the external controls, such as the quasistatic electric field or the polarization [18,19]. Moreover, they offer high electro-optical response and strong nonlinearities (higher when compared with CS₂, for example [19,20]) while maintaining a low absorption coefficient. These characteristics are important in the development of optical analog experiments, as we discuss in the next section, where we explore the analogy between light and a quantum fluid.

B. Hydrodynamic model and the Landau criteria

The analogy between light propagating in NLCs and a quantum fluid with superfluid properties can be further strengthened by introducing the hydrodynamic model that allows for a photon-fluid interpretation. This model is obtained by applying a Madelung transformation to Eqs. (1) and (2), where the envelope of the beam is written as $E = \sqrt{\rho} e^{i\phi}$ [34]. Light can then be interpreted as a fluid with density $\rho = |E|^2$ and velocity $v = \partial_x \phi$. Equations (1) and (2) can then be rewritten as hydrodynamic equations as

$$\partial_z \rho + \partial_z(\rho v) = 0, \quad (3)$$

$$\partial_z v + v \partial_x v = \frac{\partial_x}{2} \left[\frac{\partial_x^2 \sqrt{\rho}}{\sqrt{\rho}} \right] - 2\partial_x \theta, \quad (4)$$

$$v \partial_x^2 \theta - 2q\theta = -2\rho, \quad (5)$$

corresponding respectively to the Euler equations, and an equation of state for the orientation of the molecules. The first term in the second Euler equation is commonly known as the Bohm potential, or quantum pressure, and is responsible for the Heisenberg-like uncertainty. With the photon-fluid interpretation, it is possible to apply the same tools of analysis of criticality and superfluidity developed for fluids to the study of the propagation and interaction of light with NLCs. In particular, a fluid moving with velocity v can only support spontaneous excitations when they reduce the total energy of the system, namely, when the total energy of the excitation is negative:

$$E(p) + pv < 0, \quad (6)$$

where $E(p)$ is the energy of the excitation in the reference frame comoving with the fluid, and p is the linear momentum of the excitation, which can only be satisfied for fluid velocities $|v| > |E(p)/p|$. Contrarily, if the velocity of the fluid is smaller than the critical velocity given by

$$|v_c| = \min_p \left| \frac{E(p)}{p} \right|, \quad (7)$$

no spontaneous excitations appear, and the fluid has zero viscosity. This corresponds to the Landau criterion for the existence of superfluidity [41].

On the other hand, for a fluid of light, the energy and momentum of the photons are given by $E(k) = \omega(k)$ and $p = k$, respectively. Thus, the Landau criterion becomes

$$|v_c| = \min_k \left| \frac{\omega(k)}{k} \right|, \quad (8)$$

where $\omega(k)$ is the dispersion relation for light propagating in the nematic liquid crystal.

C. Small perturbations and the dispersion relation

The study of the superfluidity of a light fluid requires the knowledge of the dispersion relation $\omega(k)$, which can be obtained for small perturbations from the Bogoliubov theory [42]. According to it, the total field can be decomposed into an intense homogeneous background with amplitude A , and weaker complex envelope amplitudes $B(x)$ and $C(x)$, corresponding to the positive and negative frequency components, such that

$$E(x, z) = (A + B(x)e^{-i\omega z} + C^*(x)e^{i\omega z})e^{i\alpha z}, \quad (9)$$

where α is the propagation constant. Then, inserting Eq. (9) into Eqs. (1) and (2), assuming a zero drift velocity and linearizing the system, one obtains the dispersion relation

$$\omega(k) = \pm \sqrt{\frac{k^2}{2} \left(\frac{k^2}{2} + \frac{4A^2}{q} \frac{1}{1 + \sigma^2 k^2} \right)}, \quad (10)$$

where $\sigma^2 = v/2q$ measures the nonlocal length. Figure 1 depicts a plot of the dispersion relation for different values of parameters q and v , which could be modulated externally. This figure shows that the change in the system parameters can have a significant impact on the form of the dispersion curve. This Bogoliubov-like dispersion relation is in agreement with those obtained for similar nonlocal media [1,32]. Two regimes characteristic of superfluids can be highlighted from Eq. (10): (i) a linear regime, for low momenta, which corresponds

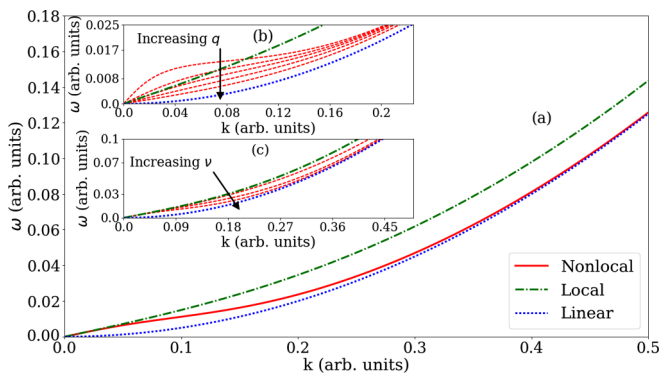


FIG. 1. Bogoliubov-like dispersion relation of the photon-fluid analog in NLCs. (a) The dispersion for the parameters $A = 0.1$, $v = 200$, and $q = 1.0$ (solid line). For comparison, the local ($v = 0$, dash-dotted curve) and the linear cases (dotted line) are also represented. The dependence of the dispersion relation on the parameters (b) q ($v = 200$) and (c) v ($q = 0.1$).

to phononlike excitations with $\omega(k) \approx \pm \sqrt{2A^2/q}k = \pm c_s k$, where c_s is the sound velocity of the medium, and (ii) a quadratic regime, which corresponds to a single-particle excitation with $\omega(k) \propto \pm k^2/2$.

Additionally, the critical velocity is calculated combining Eqs. (8) and (10). Again, two regimes can be identified: (i) if the media is highly nonlocal, i.e., $\sigma > \xi/2$ (where $\xi \equiv \sqrt{q/2A^2}$ is the typical healing length), then the critical velocity is given by

$$v_c = \sqrt{\frac{1}{\sigma} \left(\frac{1}{\xi} - \frac{1}{4\sigma} \right)}, \quad (11)$$

which is always smaller than the velocity of sound, i.e., $v_c < c_s$; otherwise, (ii) if $\sigma < \xi/2$ the critical velocity equals the sound velocity of the medium,

$$v_c = c_s. \quad (12)$$

Like in the case of thermo-optical materials [33], large nonlocal lengths σ can be a detriment to superfluidlike properties in NLCs, reducing both the effective photon-photon interaction and the critical velocity below the velocity of sound. However, NLCs can provide an additional degree of external control of the physical parameters of the system, through the control of σ . In principle, this could allow one to explore experimentally a wide range of optical analogs, either by matching the critical velocity to mimic specific superfluids, or to observe other types of superfluidlike phenomena, such as rotons, when in combination with other types of nonlinear effects [43].

In addition to the dispersion relation, the Bogoliubov theory also imposes a constraint between the Fourier transforms of the Bogoliubov modes, specifically

$$\frac{C(k)}{B(k)} = \frac{(2\omega - k^2)(vk^2 + 2q)}{8A^2} - 1 \equiv \zeta(k). \quad (13)$$

It can be noticed in Fig. 2 that for sufficiently large wave numbers, $C(k)$ tends to zero, and the Bogoliubov mode with positive frequency is dominant. However, in the deep sonic regime, this is no longer valid, as $C(k) \sim B(k)$. This result is important for a complete description of the dynamics of the optical beam and, therefore, is taken into consideration while determining experimentally the dispersion relation of the photon fluid, as investigated in the next section.

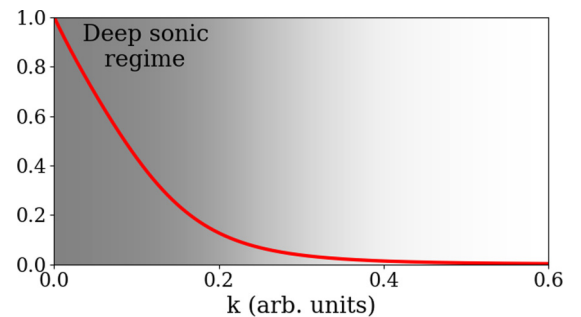


FIG. 2. $|\zeta(k)|$ as a function of the wave number, for $v = 100$, $q = 1.0$, $A = 0.1$, and $D_0 = 1 \times 10^{-8}$.

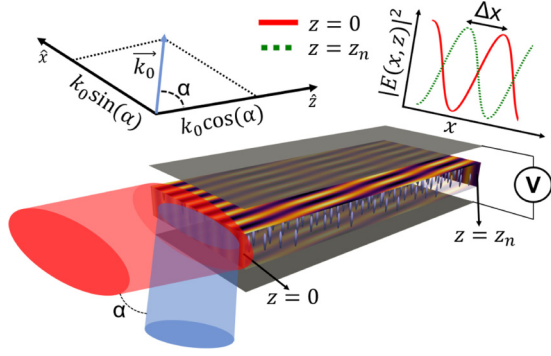


FIG. 3. Representation of the pump-probe experiment, where a flat beam interferes with a perturbation beam at the entrance of the NLC cell. The resulting beam propagates along the cell. By comparing the initial and final intensity profiles and measuring the displacement of the intensity maxima, Δx , it is possible to reconstruct the dispersion relation of the fluid of light using Eqs. (14) or (15). By varying the angle at which the beams interfere, one can change the wave number of the perturbations. Simultaneously, a quasistatic electric field applied perpendicular to the direction of propagation provides some tuning of the properties of the system.

III. PUMP-PROBE SCHEME

The dispersion relation of the fluid of light in the NLC can be determined experimentally using a pump-probe scheme, as illustrated in Fig. 3. In the figure, we represent two collimated and flat beams polarized in the y direction, with different intensities and waists. The wider and more intense beam corresponds to the uniform background A , while the narrower and less intense one creates the excitations. The two beams are made to interfere with a controllable relative angle before entering the cell filled with the NLC. This angle allows the control of the interference pattern and thus, according to the hydrodynamic description and the Bogoliubov theory, the wave number of the small-amplitude excitations. As the beams propagate inside the cell, they produce an intensity pattern along the optical axis. The dispersion relation can be obtained experimentally by determining the displacement of the intensity maxima between the input and output light patterns in the cell for different k .

This type of experiment was first proposed by Carusotto in Ref. [31] and then realized by Vocke *et al.* in Ref. [1]. However, their approach for probing the dispersion relation is limited in the deep sonic regime (small wave numbers) because they adopt an incomplete description that only considers the Bogoliubov modes with positive frequency, specifically $B(x)$ in Eq. (9). Such limitations can be overcome by considering the complete form of the Bogoliubov mode introduced in Eq. (9), which takes into account modes with both positive and negative frequencies [44].

To follow the evolution of the intensity pattern throughout the cell under the conditions of the pump-probe experiment, it is assumed that the input total field is given by $E(x, z=0) = A + D_0 e^{ikx}$. Taking D_0 as a weak perturbation, $D_0 \ll A$, this state evolves according to the Bogoliubov theory, in terms of the modes $B(x)$ and $C(x)$, following Eq. (9) and the dispersion relation (10). Figure 4 illustrates the results of numerical simulations of Eqs. (1) and (2) using standard beam

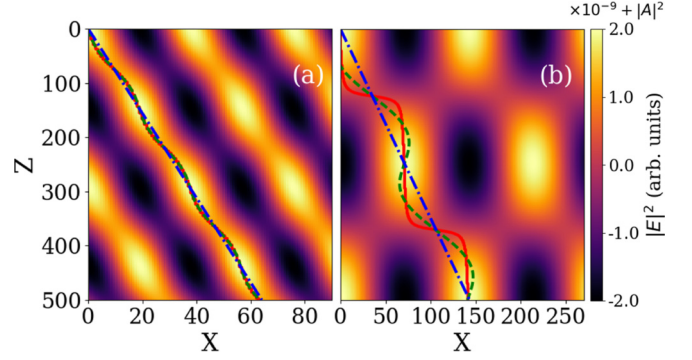


FIG. 4. Evolution of the intensity patterns of light inside the NLC cell for different regimes. (a) The typical evolution of the intensity pattern for large wave numbers and (b) the same pattern for small wave numbers, i.e., in the deep sonic regime. In both cases, the solid red line tracks the position of an intensity maximum obtained from numerical simulations, while the dashed green line describes the approximation obtained from Eq. (15). The dash-dotted blue line depicts the linear approximation provided by Eq. (14). The numerical simulations were performed by evolving the initial state $E(x, z=0) = A + D_0 e^{ikx}$ using Eqs. (1) and (2) with $A = 0.1$, $D_0 = 1 \times 10^{-8}$, $\nu = 100$, and $q = 0.1$. X and Z are dimensionless.

propagation algorithms for two initial conditions with distinct wave numbers k .

For sufficiently large k , the $C(x)$ mode is very weak and the displacement of the intensity maxima is determined essentially by $B(x)$ accordingly to a linear relation

$$x(z) \approx \frac{\omega z}{k}, \quad (14)$$

which corresponds to the method used in previous works [1]. However, when examining the deep sonic regime [see Fig. 4(b)], this linear approximation fails because the two modes $C(x)$ and $B(x)$ are comparable and the intensity maxima evolve according to

$$x(z) \approx \frac{\omega z}{k} + 2\zeta(k) \sin(2\omega z), \quad (15)$$

which must be taken into account when retrieving the dispersion relation. Indeed this expression provides a more accurate description of the evolution of the maxima along the propagation in the cell [see Fig. 4(b)]. In this regime, the method implemented previously [1] can only be used for large propagation distances, say, with $z \gg |2k\zeta(k)/\omega|$, for which relation (15) can be linearized, but that may exceed the typical size of the propagating cell.

We performed several numerical simulations of the propagation of light inside the NLC cell for a wide range of parameters ν and q , used Eq. (14) to track the displacement of the maxima in the intensity pattern, and reconstructed the dispersion relation. The results are presented in Fig. 5 and are in good agreement with the theoretical predictions in every region of the transverse momentum of the excitation, including the deep sonic regime, which confirms the accuracy of our corrected model. Moreover, to test the algorithm in conditions closer to the real experiments, we have performed the same numerical simulations with white noise up to 10% and obtained similar results (discussed in more detail in the Appendix), thus validating the experimental proposal.

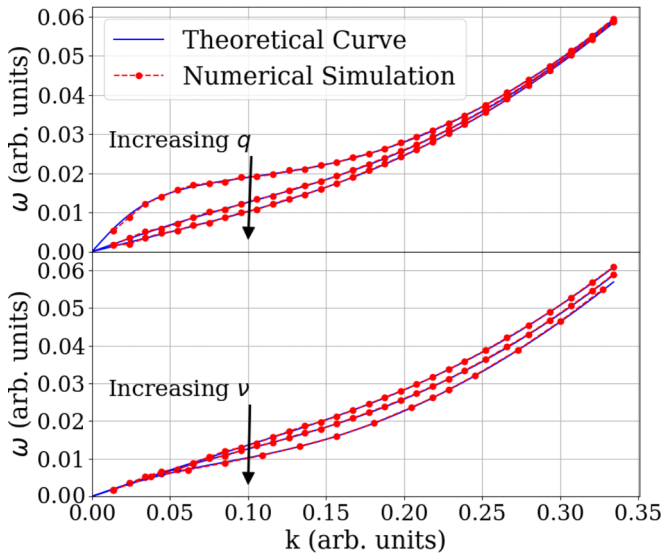


FIG. 5. Numerical simulations of the pump-probe experiment. The experiment was simulated considering large propagation distances and expression (14) was used to retrieve the dispersion relation.

IV. CONCLUSIONS

In this work, we explored theoretically the use of nematic liquid crystals in the context of optical analog experiments. Offering higher nonlinearities, with externally controllable nonlocal characteristics and with lower absorption rate when compared with the commonly used thermo-optical media, these materials can constitute tunable alternatives for the experimental realization of optical analog experiments.

Furthermore, starting from the model for an optical beam propagating in a NLC (1+1)D cell, we used the Madelung transformation to establish a hydrodynamical interpretation where light is described as a fluid. Analyzing the behavior of perturbations in the photon density, it was shown that they are characterized by a dispersion relation typical of superfluids. Following these results, we proposed a pump-probe experiment to retrieve the dispersion relation of the photon fluid in the

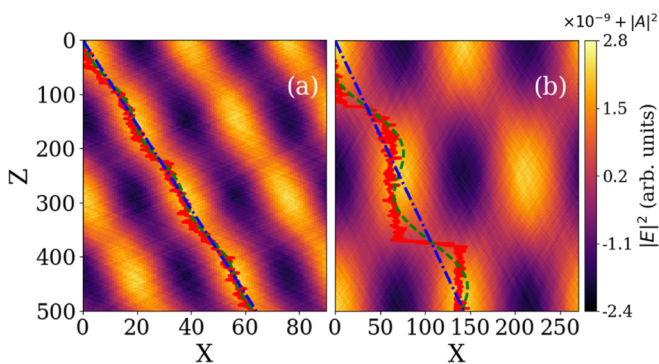


FIG. 6. Numerical results for the evolution of the intensity patterns of light inside the NLC cell. These simulations correspond to the same initial conditions and parameters used in Fig. 4 with the addition of a white noise signal of 10% on top of the perturbation. X and Z are dimensionless.

nematic liquid crystal. Employing a more complete description by taking into consideration the two Bogoliubov modes, we have provided an improved methodology that is valid even in the deep sonic regime, for short propagation distances, and can be used to provide an in-depth analysis of experiments already described in the literature.

Following the increasing interest in the literature about optical analogs, we foresee that the propagation of light in nematic liquid crystals can establish new directions of research, either in the observation of superfluid behavior of light, such as suppressed drag force, or to support a rich plethora of optical analogs of the dynamics of many-body systems, such as analog gravity models that require a medium that supports a Lorentz invariant flow (i.e., dispersionless).

ACKNOWLEDGMENTS

This work is financed by the European Regional Development Fund (ERDF) through the Operational Programme for Competitiveness and Internationalisation, COMPETE 2020 Programme, and by National Funds through the Portuguese funding agency FCT, Fundação para a Ciência e a Tecnologia, within Project No. POCI-01-0145-FEDER-032257, as well as by the North Portugal Regional Operational Programme (NORTE 2020), under the PORTUGAL 2020 Partnership Agreement. N.A.S. is supported by Fundação para a Ciência e a Tecnologia through Grant No. SFRH/BD/105486/2014. This article is based upon work from COST Action MP1403 “Nanoscale Quantum Optics,” supported by COST (European Cooperation in Science and Technology).

T.D.F., N.A.S., and A.G. contributed equally to this work.

APPENDIX

As noise is unavoidable in an actual experiment, the robustness of our method should be tested in conditions closer

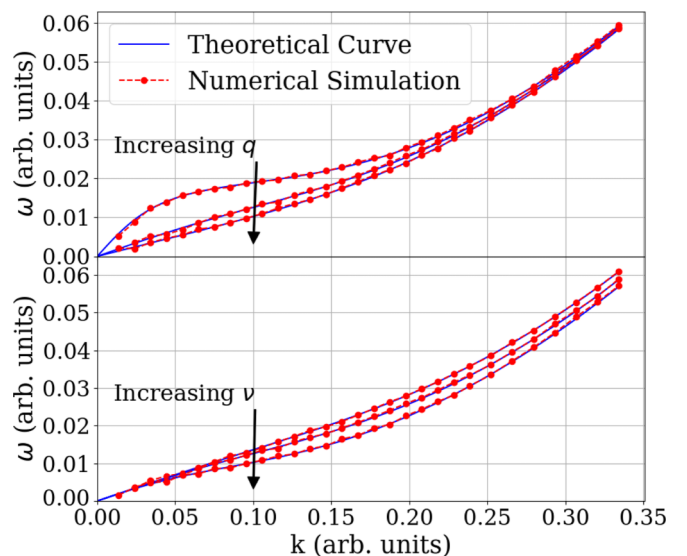


FIG. 7. Results of numerical simulations of the pump-probe experiment in the presence of noise. As in Fig. 5, the experiment was simulated considering large propagation distances and expression (14) was used to retrieve the dispersion relation.

to the ones found in the laboratory. For that purpose, we have performed the numerical simulations for the exact same range of parameters ν and q presented in Figs. 4 and 5, but with the addition of a white noise signal up to 10% on top of the perturbation. Again, the numerical simulations were performed using a standard beam propagation algorithm and the results are presented in Figs. 6 and 7. As it can be noted in the figures, in particular in Fig. 6, the noise has some effect on the results. Indeed, the existence of noise affects the accuracy in the determination of the position of the maxima and to some extent diminishes the capacity of recovering the dispersion curve. For example, the introduction of 10% noise

in the numerical experiment can perturb the position of the maxima to about one-tenth of the transverse wavelength, an acceptable trade-off under experimental conditions. However, this hindrance is limited as depicted in Fig. 7, which shows that the results obtained are in good agreement with the theoretical prediction, including in the deep sonic regime, and confirms the robustness of our method to determine the dispersion relation. If necessary, filtering techniques or other smoothing algorithms, as well as considering larger distances of propagation, can be used to improve the quality of the results by helping to reduce the loss of accuracy in the displacement of the maxima even further.

-
- [1] D. Vocke, T. Roger, F. Marino, E. M. Wright, I. Carusotto, M. Clerici, and D. Faccio, *Optica* **2**, 484 (2015).
 - [2] N. A. Silva, J. T. Mendonça, and A. Guerreiro, *J. Opt. Soc. Am. B* **34**, 2220 (2017).
 - [3] T. Roger, C. Maitland, K. Wilson, N. Westerberg, D. Vocke, E. M. Wright, and D. Faccio, *Nat. Commun.* **7**, 13492 (2016).
 - [4] A. Navarrete, A. Paredes, J. R. Salgueiro, and H. Michinel, *Phys. Rev. A* **95**, 013844 (2017).
 - [5] R. Bekenstein, R. Schley, M. Mutzafi, C. Rotschild, and M. Segev, *Nat. Phys.* **11**, 872 (2015).
 - [6] C. Barceló, S. Liberati, and M. Visser, *Living Rev. Relativity* **8**, 12 (2005).
 - [7] *Analogue Gravity Phenomenology*, edited by D. Faccio, F. Belgiorno, S. Cacciatori, V. Gorini, S. Liberati, and U. Moschella, Lecture Notes in Physics Vol. 870 (Springer International Publishing, Switzerland, 2013).
 - [8] C. C. Gan, C. M. Savage, and S. Z. Scully, *Phys. Rev. D* **93**, 124049 (2016).
 - [9] M. Peccianti and G. Assanto, *Phys. Rep.* **516**, 147 (2012).
 - [10] A. Alberucci, G. Assanto, J. Michael, L. MacNeil, and N. F. Smyth, *J. Nonlinear Opt. Phys. Mater.* **23**, 1450046 (2014).
 - [11] I. choon Khoo, *Liquid Crystals* (Wiley-Interscience, New York, 2007).
 - [12] G. Assanto, A. Fratalocchi, and M. Peccianti, *Opt. Express* **15**, 5248 (2007).
 - [13] *Nematicons: Spatial Optical Solitons in Nematic Liquid Crystals* edited by G. Assanto (Wiley, New York, 2012).
 - [14] D. Mihalache, D. Mazilu, F. Lederer, B. A. Malomed, Y. V. Kartashov, L.-C. Crasovan, and L. Torner, *Phys. Rev. E* **73**, 025601 (2006).
 - [15] Z. Xu, N. F. Smyth, A. A. Minzoni, and Y. S. Kivshar, *Opt. Lett.* **34**, 1414 (2009).
 - [16] S. Slussarenko, A. Alberucci, C. P. Jisha, B. Piccirillo, E. Santamato, G. Assanto, and L. Marrucci, *Nat. Photonics* **10**, 571 (2016).
 - [17] A. Alberucci, A. Piccardi, N. Kravets, O. Buchnev, and G. Assanto, *Optica* **2**, 783 (2015).
 - [18] M. Peccianti, A. D. Rossi, G. Assanto, A. D. Luca, C. Umeton, and I. C. Khoo, *Appl. Phys. Lett.* **77**, 7 (2000).
 - [19] M. Peccianti, A. Fratalocchi, and G. Assanto, *Opt. Express* **12**, 6524 (2004).
 - [20] M. Peccianti, K. A. Brzdakiewicz, and G. Assanto, *Opt. Lett.* **27**, 1460 (2002).
 - [21] M. Peccianti, C. Conti, and G. Assanto, *Opt. Lett.* **30**, 415 (2005).
 - [22] S. Pu, C. Hou, K. Zhan, and C. Yuan, *Phys. Scr.* **85**, 015402 (2012).
 - [23] W. Hu, T. Zhang, and Q. Guo, *Appl. Phys. Lett.* **89**, 071111 (2006).
 - [24] M. Peccianti, A. Dyadyusha, M. Kaczmarek, and G. Assanto, *Nat. Phys.* **2**, 737 (2006).
 - [25] M. Peccianti, G. Assanto, A. Dyadyusha, and M. Kaczmarek, *Phys. Rev. Lett.* **98**, 113902 (2007).
 - [26] F. Ye, Y. V. Kartashov, and L. Torner, *Phys. Rev. A* **76**, 033812 (2007).
 - [27] A. Piccardi, A. Alberucci, R. Barboza, O. Buchnev, M. Kaczmarek, and G. Assanto, *Appl. Phys. Lett.* **100**, 251107 (2012).
 - [28] A. Piccardi, A. Alberucci, N. Tabiryan, and G. Assanto, *Opt. Lett.* **36**, 1356 (2011).
 - [29] T. P. Horikis, *J. Phys. A: Math. Theor.* **48**, 02FT01 (2015).
 - [30] I. Carusotto and C. Ciuti, *Rev. Mod. Phys.* **85**, 299 (2013).
 - [31] I. Carusotto, *Proc. R. Soc. A* **470**, 20140320 (2014).
 - [32] Y. Pomeau and S. Rica, *Phys. Rev. Lett.* **71**, 247 (1993).
 - [33] D. Vocke, K. Wilson, F. Marino, I. Carusotto, E. M. Wright, T. Roger, B. P. Anderson, P. Ohberg, and D. Faccio, *Phys. Rev. A* **94**, 013849 (2016).
 - [34] E. Madelung, *Z. Phys.* **40**, 322 (1927).
 - [35] C. Michel, O. Boughdad, M. Albert, P. Élie Larré, and M. Bellec, *Nat. Commun.* **9**, 2108 (2018).
 - [36] G. Assanto, A. A. Minzoni, and N. F. Smyth, *J. Nonlinear Opt. Phys. Mater.* **18**, 657 (2009).
 - [37] C. Conti, M. Peccianti, and G. Assanto, *Phys. Rev. Lett.* **91**, 073901 (2003).
 - [38] M. Bahrani, A. Großardt, S. Donadi, and A. Bassi, *New J. Phys.* **16**, 115007 (2014).
 - [39] P. Choquard and J. Stubbe, *Lett. Math. Phys.* **81**, 177 (2007).
 - [40] K. P. Tod, *Phys. Lett. A* **280**, 173 (2001).
 - [41] I. M. Khalatnikov and I. M. Khalatnikov, *An Introduction to the Theory of Superfluidity* (Perseus, Cambridge, MA, 2000).
 - [42] L. Pitaevskii and S. Stringari, *Bose-Einstein Condensation and Superfluidity* (Oxford University Press, Oxford, U.K., 2016).
 - [43] F. Maucher, T. Pohl, S. Skupin, and W. Krolikowski, *Phys. Rev. Lett.* **116**, 163902 (2016).
 - [44] P.-E. Larre, S. Biasi, F. Ramiro-Manzano, L. Pavesi, and I. Carusotto, *Eur. Phys. J. D* **71**, 146 (2017).